Journal of the Taiwan Institute of Chemical Engineers 000 (2018) 1–8

Contents lists available at ScienceDirect

Journal of the Taiwan Institute of Chemical Engineers

journal homepage: www.elsevier.com/locate/jtice

Spinel $NiFe_2O_4$ nanoparticles decorated BiOBr nanosheets for improving the photocatalytic degradation of organic dye pollutants

Xiaowei Li[a,c,d], Haifen Xu[a], Li Wang[a], Lei Zhang[b,d,*], XiaoFeng Cao[c], YanChuan Guo[c,**]

[a] School of Chemistry and Chemical Engineering, Shandong University of Technology, Zibo, Shandong 255000, PR China
[b] School of Materials Science and Engineering, Anhui University of Science and Technology, Huainan, Anhui 232001, PR China
[c] Key Laboratory of Photochemical Conversion and Optoelectronic Materials, Technical Institute of Physics and Chemistry, Chinese Academy of Sciences, Beijing 100190, PR China
[d] Coordination Chemistry Institute, State Key Laboratory of Coordination Chemistry, School of Chemistry and Chemical Engineering, Nanjing University, Nanjing 210023, PR China

ARTICLE INFO

Article history:
Received 6 November 2017
Revised 28 January 2018
Accepted 29 January 2018
Available online xxx

Keywords:
$BiOBr/NiFe_2O_4$
Heterojunction
Photocatalysis
Magnetic separation

ABSTRACT

The BiOBr nanosheets decorated by spinel $NiFe_2O_4$ nanoparticles were successfully prepared by a simple hydrothermal approach. The structure of as-synthesized magnetically recyclable $BiOBr/NiFe_2O_4$ (denoted as BOB/NFO) composite samples consisting of different BOB/NFO mass ratios was fully characterized and the photocatalytic performance was also detailedly evaluated through degrading rhodamine B (RhB) under visible light. BOB/NFO10 (10% NFO) composite photocatalyst represented the highest catalytic efficiency, degrading 99.8% of RhB after 30 min of irradiation. The rate constant of degradation was almost 1.72 and 60.3 times as high as those of the bare BiOBr and $NiFe_2O_4$, respectively, which should be ascribed to the efficient charge separation and transfer originating from heterostructure between BOB and NFO. Radical trapping experiments showed that h^+ and $\bullet O_2^-$ played a crucial role in the photocatalytic system.

© 2018 Taiwan Institute of Chemical Engineers. Published by Elsevier B.V. All rights reserved.

1. Introduction

As is well known, solar energy is a clean and abundant energy source. With the rapid development of modern industrial economy, the efficient ultilization of solar energy for photocatalytic field towards environmental remediation and organic pollutants treatment has attracted extensive attention [1–7]. However, among the studied numerous semiconductor photocatalysts, many photocatalysts are active only under ultraviolet (about 4% of the whole solar light spectrum) irradiation, and the poor solar-light-harvesting capability seriously limits their practical applications under visible light (43% of solar light spectrum) illumination. Therefore, the design and synthesis of highly efficient and rapid visible light responsive green photocatalytic materials with good stability and low cost are still indispensable in photocatalytic technology to utilize a significant fraction of the sunlight and control environmental pollution.

Recently, numerous visible-light-driven photocatalysts have been developed for degradation of organics [8–12]. Among them, BiOBr as an important member of Bi-based photocatalysts has become a research hotspot since it has relatively low band gap energy (2.64-2.91 eV) and is thus active to visible light [13–19]. However, BiOBr also suffers from several main disadvantages such as weak visible light absorption ability and fast recombination of photogenerated electrons and holes, as well as moderate photocatalytic activity. In this regard, recent studies have demonstrated that coupling with other semiconductors to form a heterostructured nanocomposite may be an effective strategy. For example, Li et al. prepared $BiOBr/Bi_2WO_6$ composite photocatalysts through a one-pot EG (ethylene glycol)-assisted solvothermal route [20]. Photocatalytic results indicated that the as-synthesized composite samples showed significantly enhanced photo-reactivity than pure BiOBr and Bi_2WO_6 for the decomposition of rhodamine B, methylene blue and bisphenol A under the irradiation of visible light. Qiao and coworkers successfully fabricated heterojunction structure $BiOBr/Bi_{24}O_{31}Br_{10}$ nanocomposites with excellent visible light induced photocatalytic performance via a facile approach of one-step self-combustion of ionic liquids [21]. Huang's research team synthesized a core-satellite composite material with CdS particles covered on the surface of BiOBr flakes by a simple crystallization technology, which exhibited much higher

* Corresponding author at: School of Materials Science and Engineering, Anhui University of Science and Technology, Huainan, Anhui 232001, PR China.
** Corresponding author.
E-mail addresses: yutian1224@126.com (L. Zhang), yanchuanguo@mail.ipc.ac.cn (Y. Guo).

https://doi.org/10.1016/j.jtice.2018.01.043
1876-1070/© 2018 Taiwan Institute of Chemical Engineers. Published by Elsevier B.V. All rights reserved.

Please cite this article as: X. Li et al., Spinel $NiFe_2O_4$ nanoparticles decorated BiOBr nanosheets for improving the photocatalytic degradation of organic dye pollutants, Journal of the Taiwan Institute of Chemical Engineers (2018), https://doi.org/10.1016/j.jtice.2018.01.043

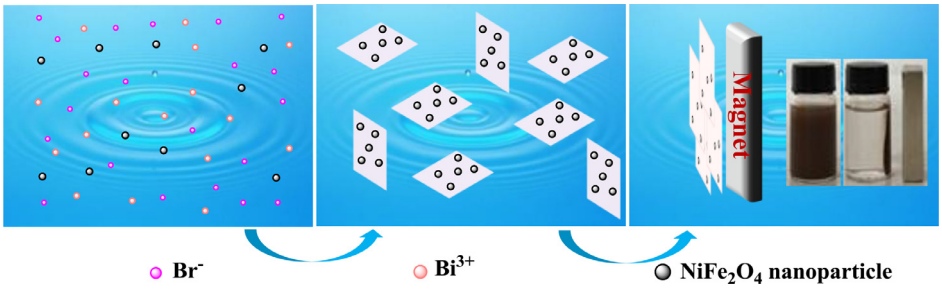

Fig. 1. Schematic illustration of the formation of the BOB/NFO nanocomposites.

photocatalytic efficiency towards bisphenol A degradation [22]. Song's group found that BiOBr/$CdWO_4$ heterojunction catalyst could be obtained using a hydrothermal process and combined with subsequent chemical precipitation method [23]. Besides these, many literatures about the construction of BiOBr-based hybrid materials with different micro/nanostructures have also been reported, such as BiOBr/$BiVO_4$ [24], BiOBr/MoS_2 [25], BiOBr/Bi_2S_3 [26], BiOBr/WO_3 [27], BiOBr/$Cd(OH)_2$ [28], BiOBr/BiOI [29], BiOBr/$CoTiO_3$ [30] and so on. At the same time, the investigation data revealed that heterostructured BiOBr-based composites could remarkably improve the photocatalytic capability of pristine BiOBr. Nevertheless, it is mentioned that these composites are difficult to separate and recover from the aqueous suspensions after a photocatalysis reaction, accordingly leading to environmental contamination and excessive economical expense. Due to this reason, the conjugation of BiOBr with magnetic semiconductors to form magnetically recyclable BiOBr-based heterojunctions can be regarded as a promising way. $NiFe_2O_4$ (NFO) as a semiconductor material has high ferromagnetic property and outstanding chemical stability, which has been coupled with other photocatalysts to achieve nanohybrids and used for the degradation of organic pollutants [31-35]. However, to the best of our knowledge, the existing reports on BOB/NFO system remain rare up to date [36–38].

In the present paper, we described the synthesis of a series of magnetically separable BOB/NFO nanocomposites with different mass ratios and their photodegradation ability for RhB. The prepared BOB/NFO photocatalysts exhibited comparatively higher visible light photocatalytic activity than that of single BiOBr and $NiFe_2O_4$. In addition, we have further analyzed the main active species during the photocatalysis and proposed the enhanced photocatalytic performance mechanism for the BOB/NFO heterostructures.

2. Experimental

All chemicals were analytical grade and used as received. Rhodamine B (RhB) was employed as model pollutants for degradation. Deionized water was used throughout the experiments. The detailed experimental contents and characterization techniques of bare BOB, NFO and BOB/NFO composite photocatalysts with different mass ratios (5%, 10% and 15%) could be found in the Supplementary material.

3. Results and discussion

The XRD patterns of individual BOB, NFO and BOB/NFO10 composite photocatalysts are displayed in Fig. 2. As for the BOB and NFO, all the detectable peaks correspond to the characteristic peaks of the tetragonal BOB (JCPDS no.73-2061) and cubic spinel NFO (JCPDS no.54-0964), respectively. Furthermore, the diffraction peaks of NFO are weaker than those of BOB, which may result from the smaller crystal size. The XRD pattern of BOB/NFO10 nanocomposite comprises the characteristic peaks of both tetragonal BOB and cubic spinel NFO without any additional crystalline phase, suggesting that BOB/NFO has only a two-phase composition and do not contain other impurity. Nevertheless, it is noted that the peaks of NFO (marked as ⋆) in the BOB/NFO10 sample are quite small because of very low ratio of NFO incorporated.

Fig. 3(a–c) reflects the morphologies and microstructures of BOB, NFO and BOB/NFO10 composite, respectively. As we can see from Fig. 3a and 3b, the size of NFO nanoparticles is in the range of 20–40 nm, while BOB has an irregular nanosheet shapes possessing smooth surface. In comparison, the surface of BOB/NFO10 is uneven due to the deposition of NFO particles onto the surface of BOB nanosheets, as follows confirmed by TEM. From the images Fig. 4, one can see that the NFO particles are uniformly and tightly loaded on BOB facet, illuminating an intimate contact between BOB and NFO. HRTEM analysis of BOB/NFO10 sample clearly displays two sets of distinct lattice fringes. One set with 0.18 nm spacing coincides with (014) crystal plane of tetragonal BOB. Other two sets 0.29 nm and 0.093 nm interplane distance are in accord with the (220) and (840) planes of cubic NFO, respectively. Associated with the discussion results of above XRD, it is concluded that BOB/NFO hybrids comprising BOB nanosheets and NFO nanoparticles have been successfully constructed. Additionally, this conclusion is also testified by EDS and elemental mappings (See Fig 3d and 3e).

The information about chemical valence of elements in BOB/NFO heterostructures is identified by means of XPS technology. As presented in Fig. 5a, the full survey spectrum of BOB/NFO10 shows the coexistence of Bi, O, Br, Fe, Ni and C, while the C element can be probably assigned to foreign carbon in the instrument. From Fig. 5b, two Bi 4f signals can be easily observed at 159.2 eV (Bi $4f_{7/2}$) and 164.6 eV ($4f_{5/2}$). Fig. 5c depicted the fine XPS spectrum of Br 3d of BOB and BOB/NFO10 sample, in which Br 3d peak with the binding energy of 68.2 eV and 69.5 eV matches with Br^-. Two peaks appeared at 529 eV and 531 eV result from oxygen in the BOB and NFO materials (Fig. 5d). The Fe 2p peaks centering at 710.6 and 723.9 eV can be attributed to Fe $2p_{3/2}$ and Fe $2p_{1/2}$, which implies that Fe exists in the form of Fe^{3+} ions (Fig. 5e). Moreover, it is evident that two 2p signals of Ni element locating at 854.8 eVans 872.7 eV belong to Ni $2p_{3/2}$ and Ni $2p_{1/2}$ in the light of Fig. 5f, respectively. These results are consistent with those gained from the previous studies [37,38].

The UV–vis diffuse reflectance spectra for as-prepared samples are tested and the corresponding curves are shown in Fig. 6. Obviously, after incorporating BOB and NFO, the absorption ability of resulted BOB/NFO composites to visible light is gradually increased with the increase of loaded NFO content. For bare BOB and NFO, the (E_g) are estimated to be 2.85 and 1.66 eV, respectively, whereas BOB/NFO heterojunctions have band gap energies ranging from 2.10–2.51 eV (See Fig. S1, Supplementary material). These properties contribute to the enhancement of photocatalytic activ-

Please cite this article as: X. Li et al., Spinel $NiFe_2O_4$ nanoparticles decorated BiOBr nanosheets for improving the photocatalytic degradation of organic dye pollutants, Journal of the Taiwan Institute of Chemical Engineers (2018), https://doi.org/10.1016/j.jtice.2018.01.043

Download English Version:

https://daneshyari.com/en/article/7104780

Download Persian Version:

https://daneshyari.com/article/7104780

Daneshyari.com